

A reduced computational effort mode-level scheme for 3D-HEVC depth maps intra-frame prediction[☆]



Gustavo Sanchez^{a,b,*}, Luciano Agostini^c, César Marcon^a

^a Pontifícia Universidade Católica do Rio Grande do Sul, Porto Alegre, Brazil

^b Instituto Federal Farroupilha, Alegrete, Brazil

^c Universidade Federal de Pelotas, Pelotas, Brazil

ARTICLE INFO

Keywords:

3D-HEVC

Intra-frame prediction

Depth maps

3D video coding

ABSTRACT

To encode the depth maps efficiently, 3D-HEVC introduced three intra-frame prediction tools: (i) Depth Intra Skip (DIS), (ii) Depth Modeling Modes (DMMs), and (iii) Segment-wise DC Coding (SDC) that raise the encoding effort. Therefore, we analyzed the most time-consuming steps at the intra-frame prediction and proposed a model-level scheme for reducing the encoding time. The most time-consuming encoding steps were the DMM-1 wedgelet search and the Rate-Distortion (RD) list evaluation in Transform-Quantization and SDC flows. Consequently, we proposed a scheme composed of two solutions for speeding up the DMM-1 and one solution for reducing the RD-list size, accelerating the RD-list evaluation. The DMM-1 speeding up solutions use the information of neighbor-encoded blocks and the data contained in the border of the encoding block to accelerate the wedgelet search. The proposed scheme reduces 31.9% the encoding time with an impact of 0.272% in the Bjontegaard Delta-rate (BD-rate), surpassing the related works.

1. Introduction

With the high demand for three-dimensional (3D) video services the 3D-High Efficiency Video Coding (3D-HEVC) [1,2] has been standardized with the objective to achieve higher compression rates and to maintain a high video quality when compared to the previous 3D video coding standards. 3D-HEVC has adopted the Multiview Video plus Depth (MVD) representation that allows obtaining better results when using view synthesis techniques [3].

Fig. 1 displays an example of MVD representation, where Fig. 1(a) contains a frame of texture and Fig. 1(b) shows its associated depth map. In MVD, each texture frame is associated with a depth map, which contains the information about the distance of the objects from the camera. The texture and depth maps are used to generate the synthesized views, and both must be compressed in the same bitstream. However, the use of only texture coding techniques tends to introduce several artifacts in the depth maps, leading to a degradation in the synthesized views quality or a low encoding efficiency. It happens because depth maps have large regions with nearly constant values (where texture algorithms are efficient) and sharp edges, which must be preserved to guarantee the synthesized views quality. In this context, the texture algorithms tend to smooth the edges, decreasing the

synthesis views quality. Therefore, the 3D-HEVC defines the use of a new set of tools to achieve higher encoding efficiency in depth maps encoding. These tools, described in the next section, are: (i) Depth Modeling Modes (DMMs) [5], (ii) Depth Intra Skip (DIS) [6], and (iii) Segment-wise Direct Component (DC) Coding (SDC) [7].

One of the most significant advances in 3D-HEVC regarding bitrate reduction and synthesized videos quality is related to depth maps intra-frame prediction where all these tools were inserted. The coding efficiency of using these new tools brings with it a significant increase in the 3D-HEVC encoder computational effort. Then, the research of solutions for diminishing the encoder computational effort, maintaining the encoding efficiency, is still a hot topic to the video coding community, which is particularly the case for applications targeting battery-based embedded systems where real-time operation and low power dissipation are essentials.

The solutions developed to reduce the 3D-HEVC encoder computational effort focus on three levels: (i) mode, (ii) block, and (iii) quadtree. The mode-level solutions aim at reducing the computational effort of a given encoding mode/step. The block-level solutions focus on skip the evaluation of a target mode if a decision criterion is met. The quadtree-level computational effort reduction targets to terminate the quadtree evaluation early or to define a limitation of the quadtree

[☆] This paper has been recommended for acceptance by Hongliang Li.

* Corresponding author at: Pontifícia Universidade Católica do Rio Grande do Sul, Porto Alegre, Brazil.

E-mail addresses: gustavo.sanchez@acad.pucrs.br (G. Sanchez), agostini@inf.ufpel.edu.br (L. Agostini), cesar.marcon@pucrs.br (C. Marcon).



Fig. 1. Kendo video sequence frame (a) texture view and (b) its associated depth map (image extracted from [4]).

depth. All these three levels of decision can be combined into a single scheme for obtaining aggressive timesaving results.

This work proposes a reduced computational effort mode-level scheme targeting the most time-consuming steps along the encoder. The developed scheme can be combined with other works that propose block-level and quadtree-level schemes to achieve even higher timesaving results.

The main contributions of this article are: (i) an analysis of the most time-demanding steps of the 3D-HEVC depth maps intra-frame prediction; (ii) a new heuristic to reduce the DMM-1 encoding time - the Pattern and Gradient-based Mode One Filter (P&GMOF); and (iii) a novel mode-level and efficient coding-aware scheme that includes three algorithms to reduce the encoding computational effort in the intra-frame prediction of 3D-HEVC depth maps with its evaluation in 3D-HEVC Test Model (3D-HTM) [8].

The remaining of this article is divided as follows. Section II explains the theoretical background of 3D-HEVC depth maps intra-frame prediction. Section IV discusses the related works. Section IV shows a motivational encoding time distribution analysis of depth maps intra-frame prediction. Section V demonstrates the algorithms that compose the proposed scheme and the motivation for their development. Section VI displays the experimental results, and Section VII concludes this work.

2. Theoretical background of 3D-HEVC depth maps intra-frame prediction

The 3D-HEVC depth maps use the same quadtree structure applied in the HEVC standard (texture only) [9]. The encoding frame is divided into many Coding Tree Units (CTUs), which are separately encoded, one by one. A CTU can be split into four Coding Units (CUs), which can be divided recursively into four CUs until reaching a minimum size and the result is a quadtree structure. A CU can be further divided into Prediction Units (PUs), where intra-frame or inter-frame prediction processes encode the blocks. In intra-frame prediction, a PU can assume block sizes from 4×4 to 64×64 , using only quadratic sizes (i.e., blocks with the same width and height) [10].

In 3D-HTM version 16.0 [8] every available block size and encoding mode should be evaluated to select the final encoder decision. The Rate-Distortion cost (RD-cost) is used in this process, and it is a function that ponders the visual quality and the required bits to represent the encoded block. Consequently, the best solution is the one that obtained the lowest RD-cost. This operation is done for texture and depth maps.

Since this article focus on the 3D-HEVC depth maps intra prediction, its related tools and operation flow will be detailed in the next subsections.

2.1. HEVC intra-frame prediction

The HEVC intra-frame prediction is also used in the 3D-HEVC depth maps. It specifies 35 prediction modes: planar, DC and 33 directional, whose directions are displayed in Fig. 2. All these modes must be evaluated to define the best one.

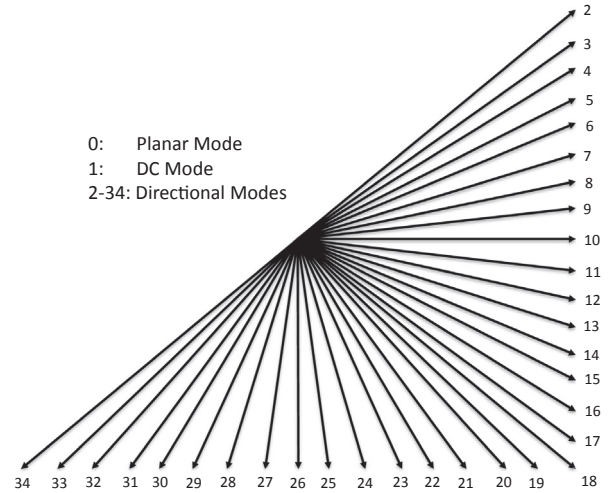


Fig. 2. HEVC Intra Prediction modes (image extracted from [13]).

3D-HTM implements a fast scheme that employs the Rough Mode Decision (RMD) and Most Probable Modes (MPM) [14] heuristics. These heuristics use a local evaluation to create a list of the modes, which have higher chance to have a competitive RD-cost. This list is called RD-list, and only the modes inside the RD-list are fully evaluated through the RD-cost.

The idea of RMD heuristic employs the Sum of Absolute Transformed Differences (SATD) to compare the available modes. Only the modes with the lowest SATDs are inserted into the RD-list. MPM gets the modes used in the encoded neighbor blocks and inserts them into the RD-list [14]. Table 1 shows the total number of directions defined by the HEVC intra prediction and the number of selected modes by RMD.

2.2. Depth Modeling modes one and four

Four Depth Modeling Modes (DMMs) were proposed for 3D-HEVC depth maps intra-frame prediction, but only two were inserted (DMM-1 and DMM-4) due to efficiency reasons [5].

The Depth Modeling Mode One (DMM-1) prediction is based on wedgelets, which are straight lines that segments blocks into two regions [5]. Fig. 3(a) presents an example of a bipartition, where a wedgelet separates the regions P_1 and P_2 .

Table 2 shows that there are many possible wedgelets defined in DMM-1, varying according to the block size. However, the 3D-HTM reference model employs by default a timesaving technique, and only a subset of the wedgelets should be evaluated. For the remaining of this article, we call as “Main Stage” the first DMM-1 evaluation. After the Main Stage, a refinement is performed evaluating at most eight wedgelets, and the best one is inserted into the RD-list. Therefore, only one wedgelet is assessed within Transform-Quantization (TQ), and SDC flows. If the DMM-1 is selected as the encoding mode in TQ or SDC flows, then additional information is inserted into the bitstream with the selected pattern, allowing the decoder to reconstruct the depth map.

Table 1
Quantity of HEVC intra modes and RMD selected modes.

Block size	HEVC intra prediction	
	Total modes	RMD selection
4×4	18	8
8×8	35	8
16×16	35	3
32×32	35	3
64×64	4	3

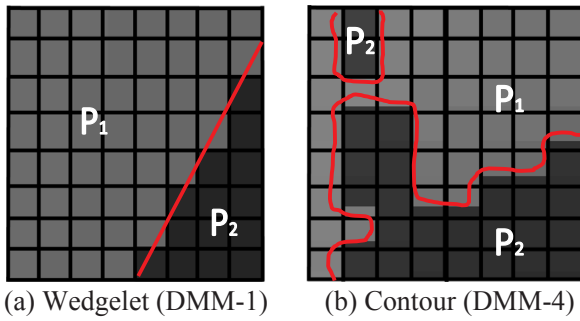


Fig. 3. Depth Modeling Modes partition.

Table 2

Total number of DMM-1 wedgelets and evaluated wedgelets in *main stage* per block size.

Block size	DMM-1	
	Total wedgelets	Main Stage wedgelets
4×4	86	58
8×8	802	314
16×16	510	384
32×32	510	384
64×64	Not allowed in this size	

The Depth Modeling Mode Four (DMM-4) applies a technique called inter-component prediction, which uses previously encoded information from the texture view during the depth map prediction to find the best contour partition.

The DMM-4 prediction dynamically creates a partition from the texture information consisting of arbitrary shapes or even disconnected regions. Fig. 3(b) exemplifies a DMM-4 partition. Since DMM-4 dynamically creates the partition, then it is not necessary to send any additional information about the partition in the bitstream, increasing the compression efficiency.

2.3. Depth intra skip (DIS)

DIS is one of the new coding tools inserted in the 3D-HEVC targeting depth maps encoding. Since large areas of the depth maps are smooth, the DIS mode can skip the residual coding in these areas, because smooth areas are not relevant for synthesized views quality. Then, DIS can reduce the bitrate of the encoded video significantly.

DIS is applied for block sizes from 8×8 to 64×64 , and four different prediction modes are allowed: (i) vertical intra prediction mode; (ii) horizontal intra prediction mode; (iii) vertical single depth mode and; (iv) horizontal single depth mode [6]. The HEVC vertical and horizontal intra directions are used to generate the first two predictions. The vertical and horizontal intra single depth modes fill the predicted block with a single depth value, which is derived from the up and left neighbor blocks, respectively.

2.4. Segment-wise direct component (DC) coding (SDC)

Instead of using only the TQ flow, the 3D-HEVC allows the usage of SDC in depth maps coding. SDC predicts the input block by (i) a single value if an HEVC intra mode is under evaluation; or (ii) two values if any DMM is under evaluation, with the goal to obtain further bitrate gains in smooth regions [7]. Therefore, it is possible to avoid the residual coding that TQ flow would require using only one single DC for HEVC intra mode or two DC values for DMMs. Moreover, to obtain further bitrate gains, a prediction in this DC values is performed using the algorithm defined in [15].

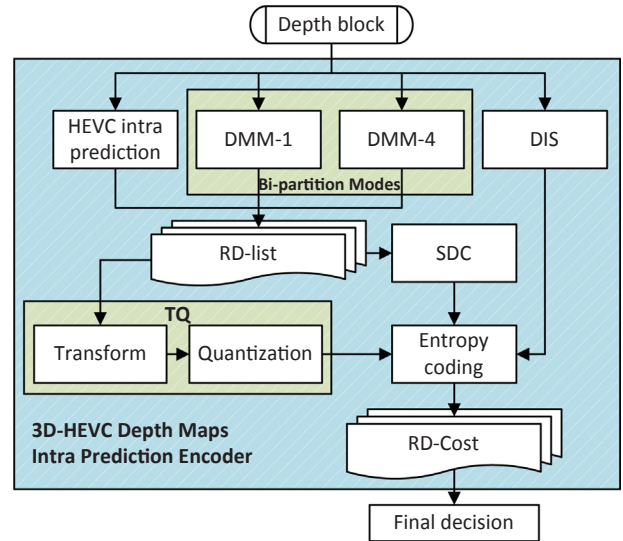


Fig. 4. Dataflow model for 3D-HEVC depth maps intra-frame prediction.

2.5. Depth maps Intra-Frame prediction flow

Fig. 4 describes the intra-frame prediction flow of depth maps. On the one hand, DIS prediction does not require residual coding, and then this tool needs only the *Entropy coding* step to obtain the RD-cost. On the other hand, an RD-list is created, where modes selected by the conventional HEVC intra prediction, DMM-1, and DMM-4, can be added to the RD-list to be later evaluated through their RD-cost.

A few of HEVC intra prediction modes are inserted in this list as explained before. However, the DMMs are not always inserted in this list since 3D-HTM employs a block-level timesaving technique by default. This timesaving technique is described in [11] and only allows the insertion of DMMs into the RD-list if the first mode in RD-list (inserted by HEVC intra prediction) is not the planar mode, and the encoding block variance is higher than a threshold, meaning that DMMs are only suitable for heterogeneous blocks.

Obtaining the RD-cost of each mode inserted into the RD-list is performed through the TQ [16] and SDC [7] steps. The TQ steps are the same applied in the HEVC, which transforms and quantifies the residual information of the predicted block, whereas SDC works as explained before. Subsequently, the *Entropy coding* step processes the TQ and SDC results.

3D-HTM employs by default a block-level timesaving technique to reduce SDC evaluation encoding time as described in [12]. The RD-cost evaluation in TQ flow is done before SDC, and the three best-encoded modes in the TQ flow are stored. If the best-encoded mode is planar or DC and the encoding block variance is lower than a predefined threshold, then only planar and DC modes are evaluated in the SDC flow. If the best-encoded mode by the TQ flow is not planar or DC, then only the three best-encoded modes are assessed according to their RD-cost in the SDC flow.

After obtaining the RD-cost of all encoding modes, the one with the lowest RD-cost is selected for that block.

3. Related work

This section presents some published works focusing on mode-level reduced computational effort scheme/algorithms for intra-frame prediction of 3D-HEVC depth maps. Some works focus on accelerating RMD and MPM selection (e.g., [17]), some other works propose to diminish the encoding time on the intra-frame prediction of the TQ and SDC flows (e.g., [18] and [19]), and others target to reduce the DMM-1 wedgelet list evaluation (e.g., [17,20], and [21]).

The work proposed by Zhang et al. [17] is capable of simplifying RMD and MPM selection, and DMM-1 wedgelet list evaluation. They classify the current block into smooth, edge, or normal, using the variance value of neighbor reference samples. Otherwise, if the block is classified as smooth, then only the planar mode is inserted into RD-list. If the block is classified as an edge, the algorithm decides the modes that should be inserted into the RD-list, according to the orientation of HEVC intra-frame direction. It also uses the orientation of DMM-1 patterns to avoid evaluating the entire DMM-1 set. If the block is classified as normal, the traditional encoding flow is performed without any simplification.

The work [18] performs mode and block level decisions. The mode-level decision always inserts into the RD-list the following modes: planar, DC, mode 10 (horizontal), mode 26 (vertical), and DMMs. It also verifies the encoding mode of the parental block (larger block that contains current block). If the planar, DC or DMMs modes do not encode its parental block, then it also inserts two additional intra-frame prediction modes into the RD-list; else, only those modes are evaluated further.

The work [19] proposed accelerating the TQ and SDC flows using mode-level and block-level decisions. The same work also introduced a new quadtree-level decision. In its mode-level decision, it evaluates only planar, DC, horizontal, vertical and MPM intra-frame prediction modes and compares its results against a threshold. The process stops when reaching a predefined threshold criterion; else, DMMs are evaluated generating a new RD-cost. If the RD-cost of DMMs is smaller than the previous RD-cost, then the process finishes. On the contrary, it computes the RD-cost for the remaining intra-frame prediction modes that share a similar direction to the best wedgelet obtained in DMM-1.

The remaining mode-level decision algorithms target on reducing DMM-1 evaluations. Sanchez et al. [20] propose a gradient filter in the borders of the block to detect the most promising positions and to evaluate DMM-1 patterns. Their work requires evaluating only wedgelets that touch the positions with high gradients values in the borders.

Fu et al. [21] reduce DMM-1 wedgelet search process by classifying the encoding block according to the variance of many regions of this block. This classification allows searching only for wedgelet patterns with similar orientations.

4. Encoding time distribution analysis

This article aims at reducing the computational effort of the most time-consuming encoding tools involved in the intra-frame prediction of 3D-HEVC depth maps coding. The first investigation targets an analysis of the encoding time distribution among each encoding step for depth maps intra-frame prediction.

The experiments consider the Common Test Conditions (CTCs) defined by the 3D-HEVC community [4]; they include eight videos of different resolutions processed by the 3D-HTM, considering the QPs pairs (QP for texture – QP for depth maps): 25–34, 30–39, 35–42, and 40–45. The experiments select all-intra for encoder configuration since this article emphasis on the intra-frame prediction.

This encoding time evaluation considers the following steps: (i) RMD and MPM selection; (ii) DMM-1 wedgelet search; (iii) DMM-4 pattern generation; (iv) RD-list evaluation in the TQ and SDC flow; and (v) DIS evaluation. The steps (iv) and (v) also consider the encoding time spent in the *Entropy coding* as performed in our previous work [22].

Fig. 5 reveals the encoding time distribution among these encoding steps for each block size, regarding the depth maps corner QPs. Notice that 4×4 blocks do not present DIS and SDC since these modes are applied in block sizes ranging from 8×8 to 64×64 . Besides, DMM-1 and DMM-4 are not shown in 64×64 blocks because DMMs are applied for block sizes ranging from 4×4 to 32×32 .

The three most time-consuming steps are the DMM-1 wedgelet search and the RD-list evaluation in TQ and SDC. The encoding time of

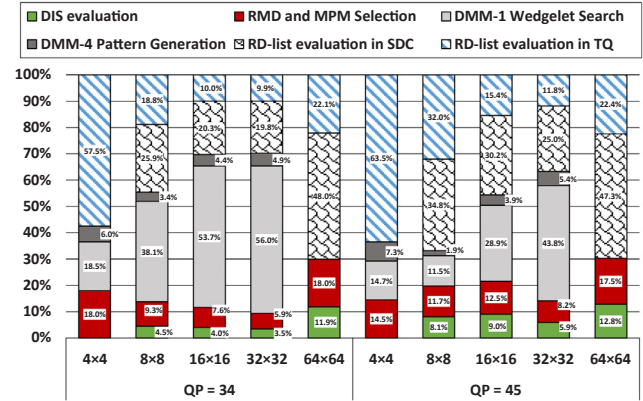


Fig. 5. Encoding time distribution for depth maps intra-frame prediction.

these three operations together ranges between 69.74% and 85.73%, regarding the block size and QP.

Concerning 4×4 blocks, the encoding time of these three operations is 75.97% (QP = 34) and 78.21% (QP = 45). For both QPs, the RD-list evaluation in the TQ flow is the most time-consuming operation, varying from 57.5% to 63.5% of the total depth maps intra-frame prediction. DMM-1 has the second highest computational effort ranging from 14.7% to 18.5%.

For blocks from 8×8 to 16×16 , the grouped encoding time of those three steps is 82.82% (8×8 and QP = 34), 84.04% (16×16 and QP = 34), 78.31% (8×8 and QP = 45), and 74.56% (16×16 and QP = 45). In this block range, the DMM-1 is the most time-consuming step with low QPs, whereas, with higher QPs, SDC becomes the operation with the highest encoding time. It happens, since the heuristic applied by default in 3D-HTM, which was proposed in [11], reduces the number of DMMs evaluation according to the used QP. Therefore, when using low QPs, there will be fewer skipped DMMs. In all of these cases, the TQ evaluation also has a considerable encoding time, occupying the third place in this criterion.

For 32×32 blocks, the grouped encoding time of DMM-1, TQ and SDC evaluations represents 85.73% for the lowest QPs and 80.55% for the highest QPs. In these cases, the DMM-1 has the highest encoding time independently of QP. It occurs because the heuristic presented in [11] removes the DMMs evaluation of the low variance block. Since larger blocks tend to have higher variance, then fewer DMMs are skipped. The second higher encoding time was obtained in the SDC evaluation, and the third higher encoding time was attained in the TQ flow evaluation.

When 64×64 blocks are processed, the scenario is similar for different QPs, and the SDC evaluation is the most time-consuming operation, representing almost 50% of the total computational effort. In this block size, the second higher encoding time was obtained in the TQ flow evaluation. Therefore, one can conclude that the DMM-1, the RD-list evaluation in TQ, and the RD-list evaluation in SDC should be the main target for achieving efficient solutions for computational effort reduction on mode-level.

5. Mode-level decision scheme – motivation and configuration setup

This section presents the designed mode-level decision scheme, which is composed of three algorithms: (i) DMM-1 Fast Pattern Selector (DFPS), (ii) P&GMOF and, (iii) Enhanced Depth Rough Mode Decision (ED-RMD). P&GMOF and DFPS focus on reducing the encoding time in the DMM-1 pattern generation, while ED-RMD focuses on reducing the TQ and SDC evaluations. The targeted encoding steps are the most time-demanding inside an all-intra 3D depth maps encoder, as previously demonstrated.

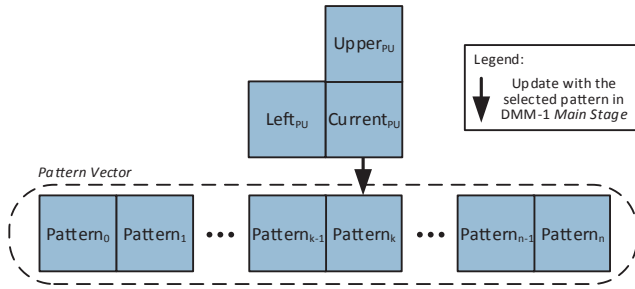


Fig. 6. Example of neighbor PUs and selected patterns in the Main Stage of DMM-1.

5.1. DMM-1 Fast pattern Selector (DFPS)

The DFPS algorithm was designed in our previous work [23] and intends to use the DMM-1 pattern selected by the neighbor PUs, to define the pattern of the current PU quickly. DFPS uses a Pattern Vector, which is initially filled with zeros. Let $Pattern_{up}$, $Pattern_{left}$ and $Pattern_{curr}$ be the pattern selected by the upper, left and current PU in the Main Stage of DMM-1, respectively. At the end of the Main Stage of DMM-1 of the current PU, the selected pattern number ($Pattern_{curr}$) is inserted into the corresponding vector position, as presented in Fig. 6.

P_{copy} is a predictor that reuses the DMM-1 pattern of the neighbor PUs, and P_{extend} is a predictor that extends the DMM-1 direction of the neighbor PUs. P_{copy} indicates the pattern with the smallest distortion between copying $Pattern_{left}$ and $Pattern_{up}$ for the current PU. P_{extend} indicates the pattern with the smallest distortion among extended wedgelet orientation of $Pattern_{left}$ and $Pattern_{up}$. The main idea is to correlate the decisions of previous evaluated neighbor PUs with the current PU evaluation. When evaluating the K^{th} $Current_{PU}$ in the row, the pattern selected by the $Left_{PU}$ is stored in the position $Pattern_{k-1}$ and the pattern selected by the $Upper_{PU}$ is stored in position $Pattern_k$ in the Pattern Vector. Therefore, by accessing the Pattern Vector, the $Current_{PU}$ can be encoded retrieving the necessary information for the prediction based on P_{copy} and P_{extend} . At the end of the encoding, the DMM-1 pattern selected for $Current_{PU}$ is written in $Pattern_k$, since the pattern selected by the $Upper_{PU}$ is not necessary anymore for the prediction of any other pattern. Then, when evaluating the next PU ($K + 1$), the necessary information for its prediction are available in the Pattern Vector in the positions $Pattern_k$ and $Pattern_{k+1}$.

We analyze the success rate of each predictor according to the block size for every video sequence of the CTC. The success rate means the number of cases the proposed predictors had success (i.e., its prediction was the same of Main Stage) divided by the total number of evaluations. This experiment only evaluates P_{extend} when P_{copy} fails. Fig. 7(a) and (b) illustrate the success rate of each predictor for block sizes of 4×4 and 32×32 , respectively, considering the average values of all evaluated QPs defined in CTC.

These results show that smaller PUs obtain higher success in P_{copy} , while larger PUs obtain better results in P_{extend} .

Fig. 7(c) depicts the total success rate of all available block sizes and represents the union of both predictors success rate (i.e., considering that any of the predictors had success), which is a relevant information when combining these predictors in a single solution. This analysis allows concluding that the combination of both predictors brings a high success rate, independently of the encoding block size.

Along with this analysis, Fig. 8 presents the probability density function of having success in P_{copy} according to the obtained distortion divided by the block size, which is a normalization used as a criterion since larger block sizes tend to have larger distortion values. This function, which follows a Gaussian distribution, was achieved executing the GT_Fly video sequence under all-intra configuration. Small distortion values tend to result in higher success rate, while higher values of distortion tend to fail the P_{copy} prediction.

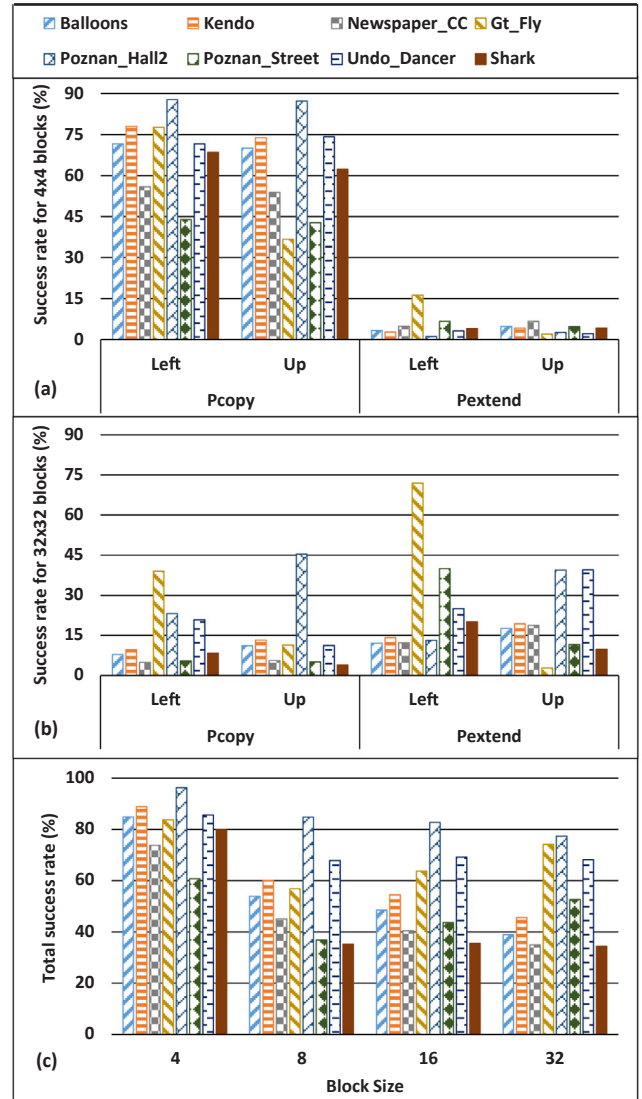


Fig. 7. The success rate of P_{copy} and P_{extend} for (a) 4×4 and (b) 32×32 blocks, and (c) the total success rate for all available block sizes.

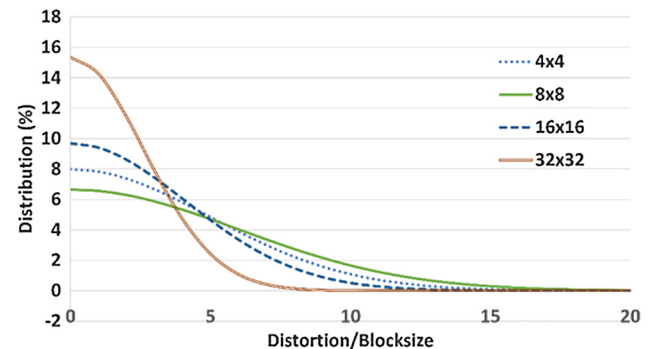


Fig. 8. Probability density function of having success in P_{copy} .

The normalized values obtained by the predictors have a direct relation with the predictor success or fail probabilities. Therefore, the predictors can be used to perform an early termination on the DMM-1 evaluation, according to a threshold criterion. The same analysis has been performed for P_{extend} resulting in similar conclusions. Fig. 9 shows the dataflow model of the DFPS algorithm together with the DMM-1 encoding algorithm. Looking for a lightweight solution, capable of

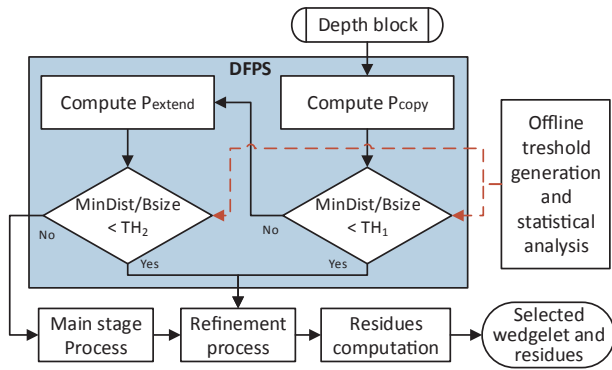


Fig. 9. DFPS dataflow model inside the DMM-1 algorithm.

skipping many DMM-1 evaluations, DFPS starts finding the minimum distortion in P_{copy} performing at most two pattern evaluations. If the normalized value is lower than the threshold TH_1 , then finalizes the *Main Stage* of DMM-1, and the refinement is performed followed by the residue computation.

Further evaluations are required to obtain a reliable prediction on DMM-1 *Main Stage* when TH_1 criterion is not met. Therefore, instead of evaluating the entire DMM-1 initial set, a medium-weight solution is designed, where P_{extend} is evaluated extending left and upper PUs wedgelets orientation. Subsequently, the normalized value is compared with TH_2 , which is a second predefined threshold. If it is smaller than the TH_2 , then the algorithm skips the *Main Stage* performing the *Refinement Stage*. Otherwise, further evaluations are required, and the remaining wedgelets are reevaluated in the *Main Stage* without any simplification.

The threshold values lead to light or aggressive solution regarding the percentage of skipped patterns. Thus, we evaluated 16 scenarios to understand the impact of threshold variation. All combinations using $TH_1 = \{1, 6, 11, 16\}$ and $TH_2 = \{2, 27, 52, 77\}$ were evaluated in our previous work [23] aiming to find a good tradeoff between the percentage of skipped patterns and encoding efficiency in terms of Bjontegaard Delta-rate (BD-rate) [25]. The evaluated thresholds were defined based on the average and the standard deviation obtained in the experiment demonstrated in Fig. 8, and a similar analysis was used for P_{extend} .

Fig. 10 displays the percentage of wedgelets reduction according to the BD-rate criterion, when evaluating 10 frames of the GT_Fly video sequence under all-intra configuration. Here, only 10 frames of GT_Fly video sequence were evaluated to avoid setting up the operation point based on the characteristics of all videos in CTCs. Then, next Section presents an evaluation of all videos in CTC showing the operation point is not overtrained.

DFPS allows some operation points that provide better coding effectiveness or higher number of skipped patterns. Fig. 10 highlights the operation point selected in this article: $TH_1 = 6$ and $TH_2 = 2$. In this

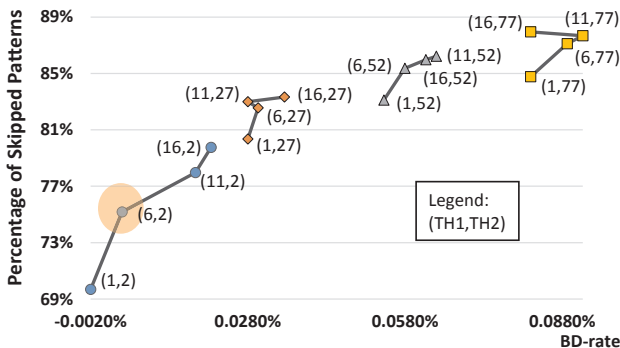


Fig. 10. Threshold evaluation for DFPS algorithm.

case, the BD-rate impact is only 0.004%, and the skipped patterns are 75.17%. This operation point was selected because it allowed a significant reduction in the wedgelets evaluation with negligible loss in the BD-rate results. The other evaluated points or caused a higher increase in the BD-rate or presented a lower reduction in the evaluated patterns. Therefore, the chosen operation point provided a good tradeoff between patterns skipped and BD-rate. However, other operation points can be used if the designed system requires a higher percentage of skipped patterns or a lower impact on the encoding efficiency.

When using DFPS, only a single wedgelet is evaluated in the best case (only P_{copy} is analyzed, and the upper and left PUs have selected the same wedgelet). In the worst case (i.e., no simplification is performed), the RD-costs calculated by DFPS is the same than the traditional approach. Moreover, according to this simulation, the proposed solution can reduce more than 75% the wedgelets evaluation, on average.

Several works in the literature use information of neighbor PUs to accelerate the current PU evaluation in HEVC standard; however, none of them assessed how to speed up the DMM-1 evaluation based on this information. Another innovation of this work is that the designed solution always stores the information of the DMM-1 *Main Stage* pattern in a vector. Consequently, even if other coding tools have been selected in the complete RD-cost evaluation, the DMM-1 information of each PU is stored and can be used to accelerate the encoding process of the next PUs. Other works in literature use only the information of the encoded PU to speed up the encoding process, and we designed the *Pattern Vector* that stores the information even when the DMM-1 is not selected to encode the PU, which also speeds up the DMM-1 calculation of the next PUs.

5.2. Pattern and gradient-based mode one Filter (P&GMOF)

Since the DMM-1 algorithm is one of the most time-consuming steps in depth maps intra-frame prediction, our previous work [20] has proposed the Gradient-based Mode One Filter (GMOF) algorithm to reduce the number of evaluated wedgelets. It reduces the number of wedgelets by searching for wedgelets whose straight line starts in a position that there is a considerable high change of gradient value (i.e., the difference between two consecutive pixels) in the block borders. The solution proposed in our previous work is line-based because it considers the position of the stored straight line.

Fig. 11 exemplifies an 8×8 depth block with the selected wedgelet and the block borders gradient values when the DMM-1 algorithm is applied. Notice that the best-encoded wedgelet found in this example is near to the positions with the highest gradient. Consequently, one can conclude, that the border positions with high gradient values tend to be good candidates for the DMM-1 wedgelet decision process.

The original line-based GMOF algorithm creates a gradient list with N positions ordered by the highest gradients of the borders. The positions in this list point to the position change that obtained that gradient, as presented at the bottom of Fig. 11. The algorithm evaluates only wedgelets whose straight line is located in these positions. Applying intense experimentation, the best N selected in [20] was eight.

After this initial evaluation, GMOF applies the original DMM-1 refinement, which unfortunately often does not reach the best wedgelet approximation. Fig. 12 exemplifies the encoding of a 4×4 depth block with the best pattern selected by the original DMM-1 algorithm. Notice that the best wedgelet pattern is obtained starting the wedgelet in an intermediary pixel and there is a gradient value only a half pixel of distance from there. It occurs because the DMM-1 wedgelets evaluations are stored in a pattern-based way, and not line-based as that previous work explored.

Fig. 13 depicts the dataflow model of P&GMOF that is a new pattern-based GMOF algorithm proposed for taking into account that the DMM-1 evaluation does not use the wedgelet line position, but only the binary pattern.

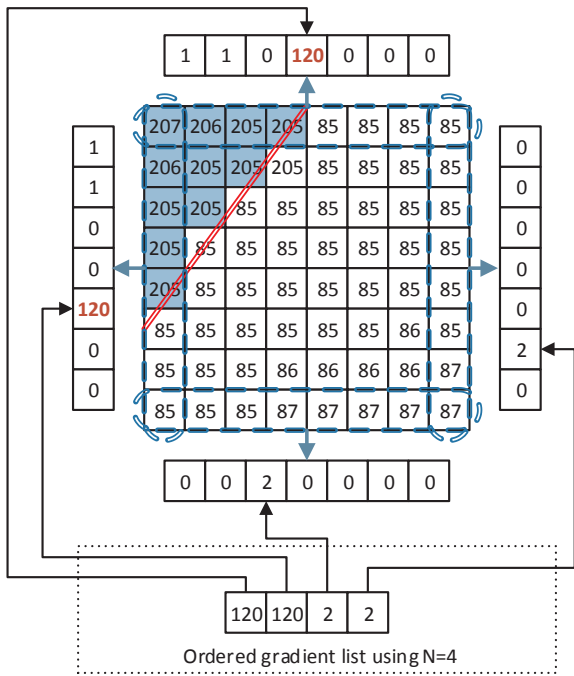


Fig. 11. An 8 × 8 depth block with the gradient of its borders and the selected wedgelet in the DMM-1 Main Stage process.

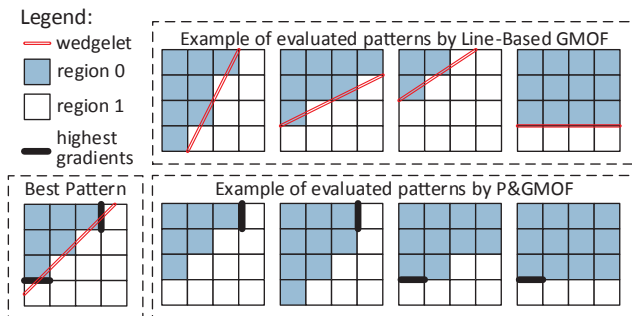


Fig. 12. Threshold evaluation for the DFPS algorithm.

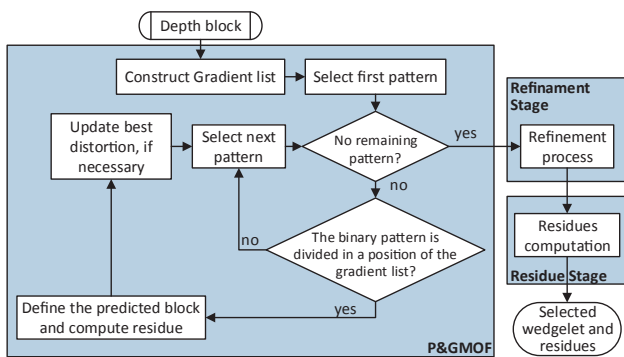


Fig. 13. P&GMOF dataflow model.

This algorithm maintains the gradient list constructed by the original line-based GMOF. After constructing this list, the pattern of each wedgelet in the initial wedgelet pattern set is analyzed with the positions in the gradient list. If there is a division in the pattern in any of these positions (i.e., it changes from one region to another in that position), the wedgelet is evaluated regarding its RD-cost. Otherwise, the next wedgelet is applied to the same process. Furthermore, when the entire initial wedgelet set is analyzed, the original refinement is applied, and the wedgelet that obtained the lowest RD-cost is selected as

the best-encoded wedgelet, sending its residues and encoding information to the next encoder modules.

The same example presented in Fig. 12 for line-based GMOF is also presented for P&GMOF. In this case, the pattern-based version is capable of achieving the same wedgelet that would be selected by the original DMM-1 algorithm. P&GMOF is capable of achieving the same timesaving reduction obtained by the traditional GMOF; however, now a better wedgelet approximation is achieved and therefore the encoded depth map quality should be enhanced. Moreover, with a better depth map quality, the higher quality synthesized views can be obtained.

5.3. Enhanced depth Rough mode decision (ED-RMD)

The ED-RMD heuristic was designed in our previous work [24]. The RD-list evaluation in both TQ and SDC flow is a time-consuming task because all modes inserted into RD-list should be evaluated in both flows. Therefore, we developed the ED-RMD heuristic that reduces the RD-list size resulting in a significant reduction in the computational effort.

The development of ED-RMD heuristic considered the results of encoding of all videos inside CTC using the corners QPs for depth coding in all-intra configuration. We stored the best directional mode selected during each block computation, and we compared its RD-cost with its position in RMD rank or MPM decision.

Fig. 14 shows the percentage of cases that the RMD best-ranked mode, the second RMD best-ranked mode, the first MPM, the second MPM, and the remaining modes are selected by the encoder decision for QP-depth equal to 34 and 45. The legend *Others* in Fig. 14 groups all the cases when the encoding decision used other RMD modes than those highlighted in this figure. Notice that the first RMD mode represents more than 50% of the selections in all encoding cases; and, the selections of the first RMD rise when increasing the encoding QP-depth. Even so, the second RMD mode and the first MPM have a significant quantity of selections, which rises with the growth of the block size.

One can conclude from this analysis that depth maps coding does not require the complete RD evaluation for all modes inside RD-list. It happens because the RMD and MPM were designed considering texture coding that contains a more complex behavior. Besides, due to many modes inserted into depth maps intra-frame prediction, the removal the RD evaluation of some HEVC intra-frame prediction modes can reduce the encoding time significantly without considerable impacts on the coding efficiency.

We performed 48 experiments to identify the encoding efficiency and computational effort impact of the proposed ED-RMD heuristic, considering that many encoding modes selected by RMD and MPM heuristics have almost no impact in the encoding selection. These experiments encoded ten frames of Balloons and Undo_Dancer sequences under the all-intra configuration.

Tables 3 and 4 present the results of the experiments using one and two MPMs, respectively. In these tables, ET represents the percentage of encoding time compared with the 3D-HTM execution. Notice that

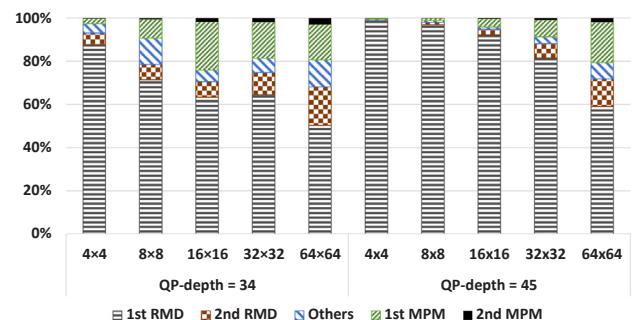


Fig. 14. Statistical usage of the RD-list position according to the block size.

Table 3
ED-RMD evaluation using one MPM.

Modes selected for 4×4 and 8×8	Modes selected for 16×16 to 64×64					
	1		2		3	
	BD-rate	ET	BD-rate	ET	BD-rate	ET
8	0.164%	90.2%	0.072%	95.5%	0.043%	99.3%
7	0.146%	87.8%	0.120%	92.7%	0.052%	97.0%
6	0.219%	85.1%	0.159%	90.4%	0.097%	94.5%
5	0.223%	82.6%	0.143%	87.7%	0.109%	91.9%
4	0.290%	80.2%	0.206%	85.3%	0.175%	89.5%
3	0.380%	77.6%	0.263%	82.7%	0.239%	87.0%
2	0.440%	74.9%	0.407%	80.1%	0.326%	84.2%
1	0.577%	71.4%	0.455%	76.4%	0.451%	80.5%

Table 4
ED-RMD evaluation using two MPMs.

Modes selected for 4×4 and 8×8	Modes selected for 16×16 to 64×64					
	1		2		3	
	BD-rate	ET	BD-rate	ET	BD-rate	ET
8	0.108%	90.7%	0.050%	95.8%	0.000%	100.0%
7	0.103%	88.3%	0.053%	93.5%	-0.002%	97.7%
6	0.149%	85.9%	0.136%	91.0%	0.020%	95.3%
5	0.176%	83.3%	0.128%	88.4%	0.068%	92.6%
4	0.248%	80.8%	0.194%	86.1%	0.120%	90.2%
3	0.365%	78.4%	0.274%	83.5%	0.235%	87.7%
2	0.432%	75.5%	0.347%	80.7%	0.280%	85.0%
1	0.558%	71.7%	0.478%	77.1%	0.397%	81.3%

removing one intra-frame mode from larger block sizes implies in higher computational effort reduction than removing one mode from smaller block sizes. Moreover, removing one evaluation of MPM implies in a small computational reduction and a negligible impact on BD-rate. Consequently, in real-time systems, reducing the MPM evaluation to a single mode results in a sound tradeoff.

These experiments allow concluding the computational effort reduction depends on the system configuration. Notice that there is no optimum configuration for the proposed algorithm, and the system should be configured according to its application constraints such as maximum BD-rate, encoding time, and maximum power dissipation. If a higher encoding efficiency is desired, then a larger number of modes can be inserted into the RD-list; however, when requirements of minimizing the encoding time or power dissipation are more important, fewer modes can be inserted in the RD-list with small impact on the encoding efficiency.

The ED-RMD heuristic was defined using the four best-ranked modes in RMD and one MPM for 4×4 and 8×8 blocks, and only the best-ranked mode in RMD and one MPM for 16×16 to 64×64 blocks, considering the analysis explained before. Other operation points could also be explored, but this configuration presented the best tradeoff between computational effort reduction and coding efficiency degradation. The selected configuration was capable of reaching a time-saving of almost 20%, with a BD-rate increase under 0.3%, which is a considerable computational effort reduction and a negligible impact on the encoding efficiency. These results are better discussed in the next section.

6. Results and comparisons

Table 5 illustrates the results acquired with the individual evaluation of the three algorithms that compose our reduced computational effort mode-level scheme in 3D-HTM version 16.0 under all-intra configuration, following CTC for 3D experiments [4]. In average, the DFPS

solution can save 11.7% in the global 3D-HEVC encoder encoding time (texture and depth map encoding), with a drawback of 0.0467% in BD-rate.

We evaluated P&GMOF using $N = 8$ since this value was already studied in our previous work [20]. This algorithm can achieve a global 3D-HEVC encoder timesaving of 6.5% with a BD-rate increase of 0.0119%. Notice that DFPS and P&GMOF can be applied together for reducing the DMM-1 computational effort because instead of evaluating the remaining patterns when the P_{extend} predictor fails, it is possible to evaluate only the positions indicated by P&GMOF.

For a better interpretation of these timesaving results, Fig. 15 shows the percentage of wedgelets skipped for P&GMOF and DFPS, according to the evaluated video sequence. On average, P&GMOF and DFPS reduce 58% and 71% the wedgelets evaluation, respectively. The highest DFPS gains are obtained for higher resolution videos because the first predictor succeeds more often in this kind of videos. Although P&GMOF and DFPS obtain similar average reduction in wedgelets evaluations of lower resolution videos, the superior timesaving reduction of DFPS is explained because it can save more the computational effort spent in smaller block sizes than P&GMOF.

This section evaluates the proposed ED-RMD heuristic employing the full CTC since Section V.C only used a subset of the CTCs specifications. The results show a timesaving of 20.6% in the global encoder with a drawback of 0.1671% in BD-rate of synthesized views, on average. This timesaving was obtained because the HEVC intra-frame prediction modes in RD-list was reduced by 50% in 4×4 and 8×8 PUs, and by 66% in the remaining PU sizes. Therefore, the TQ and SDC evaluation encoding effort was proportionally reduced.

Our mode-level scheme combines the DFPS, P&GMOF and, ED-RMD for reducing the encoding computational effort. It uses ED-RMD without requiring any modification; however, P&GMOF is used only when DFPS must encode the entire wedgelet list; and, instead of evaluating the entire list, the P&GMOF performs the final evaluation. Therefore, the designed scheme applies DFPS and P&GMOF for reducing the computational effort in the DMM-1 pattern generation. Besides, it reduces the RD-list evaluation in TQ and SDC flows by reducing the RD-list size using ED-RMD.

Table 6 shows the evaluation results for our mode-level scheme under CTC of the 3D-HTM 16.0 with all-intra configuration.

The proposed scheme saves 31.9% of encoding time considering the whole encoder operation (includes texture and depth maps) with a drawback of a BD-rate increase of 0.255%. If only depth maps coding is considered, then it is possible to reduce 37.4% the execution time.

Fig. 16 displays the resulting encoding time of the system compared to the 3D-HTM encoding time, according to the encoding QP for the eight video sequences. Notice that the proposed mode-level scheme reduces the computational effort of the four evaluated QP-depth values considerably.

This scheme reduces the effort spent in the most time-consuming steps in the 3D-HEVC depth maps intra-frame prediction (DMM-1 pattern generation, RD-list evaluation in TQ, and RD-list evaluation in SDC) significantly and with minor impact on the encoding efficiency.

To exemplify the visual effects of this scheme, Fig. 17 shows the first frame of a synthesized view in Poznan_street video sequence using the original 3D-HTM 16.0 in Fig. 17(a) and the modified 3D-HTM using the mode-level decision in Fig. 17(b). This view was synthesized in the intermediary position between the central and the left view of the scene. One can observe that the minor impacts in coding efficiency did not cause any perceptible differences in the quality of the synthesized views.

Table 7 aims to compare the experimental results with some related works. One can see, it is not possible to make a precise comparison of our work with the related works because they were implemented into different versions of 3D-HTM. However, the encoding efficiency and the timesaving variations from distinct versions of the 3D-HTM tends to have a low significance when percentages values are considered.

Table 5
Individual results of the proposed algorithms.

Resolution	Videos	DFPS [23]		P&GMOF		ED-RMD	
		Synthesis only BD-rate	Timesaving	Synthesis only BD-rate	Timesaving	Synthesis only BD-rate	Timesaving
1024 × 768	Balloons	0.0152%	8.1%	0.0158%	6.8%	0.2662%	19.9%
	Kendo	0.0189%	6.5%	0.0141%	5.1%	0.2844%	19.4%
	Newspaper_cc	0.0733%	10.8%	0.0344%	6.6%	0.3064%	20.3%
	Average	0.0358%	8.5%	0.0214%	6.2%	0.2857%	19.9%
1920 × 1088	Gt_fly	0.0045%	15.3%	0.0049%	8.3%	0.0965%	21.0%
	Poznan_hall2	0.1847%	13.3%	−0.0018%	6.1%	0.2046%	22.0%
	Poznan_street	0.0380%	14.6%	0.0051%	7.2%	0.1484%	22.7%
	Undo_dancer	0.0298%	13.7%	0.0107%	5.7%	0.0974%	19.0%
	Shark	0.0152%	11.0%	0.0049%	8.3%	0.0829%	20.3%
	Average	0.0533%	13.6%	0.0047%	6.8%	0.1367%	21.0%
Average		0.0467%	11.7%	0.0119%	6.5%	0.1671%	20.6%

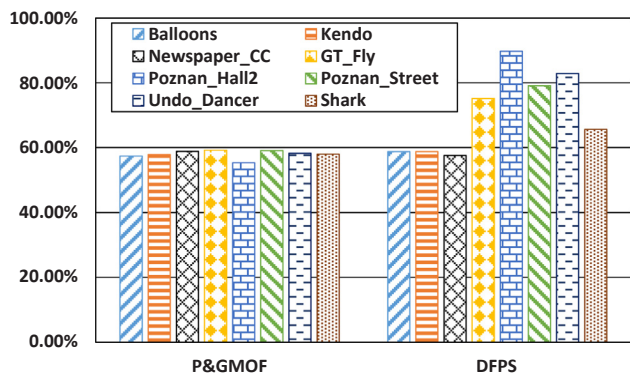


Fig. 15. Wedgetlets evaluation reduction with P&GMOF and DFPS algorithms.

Table 6
Results of our mode-level scheme.

Videos	Model-level complexity reduction		
	Synthesis only BD-rate	Encoding timesaving	Depth timesaving
Balloons	0.357%	29.6%	34.1%
Kendo	0.371%	28.8%	33.9%
Newspaper_cc	0.460%	31.0%	35.4%
Gt_fly	0.116%	34.7%	40.6%
Poznan_hall2	0.427%	32.5%	38.8%
Poznan_street	0.217%	36.1%	41.7%
Undo_dancer	0.118%	32.1%	38.5%
Shark	0.107%	30.6%	36.2%
Average	0.272%	31.9%	37.4%

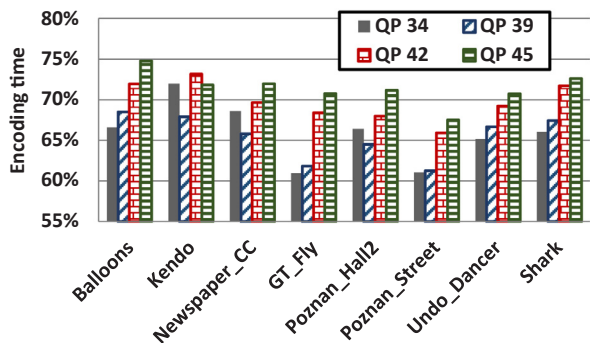


Fig. 16. Encoding time achieved by the reduced computational effort mode-level scheme compared to 3D-HTM, according to QP.



(a) original 3D-HTM



(b) the mode-level scheme

Fig. 17. Subjective quality of the synthesized view by the (a) original 3D-HTM and (b) the mode-level scheme in Poznan_street video sequence.

Table 7
Comparisons with related work.

Work	Decision level	BD-rate	Timesaving on Encoding	
			DMM-1	
This work – 3D-HTM 16.0	Mode	0.27%	31.9%	–
Zhang [17] – 3D-HTM 8.1	Mode	1.03%	27.9%	–
Zhang [18] – 3D-HTM 13.0	Mode and block	0.54%	32.9%	–
Peng [19] – 3D-HTM 13.0	Mode and quadtree	0.8%	37.6%	–
Sanchez [20] – 3D-HTM 7.0	Mode	−0.05%	1.7%	–
Fu [21] – 3D-HTM 8.1	Mode	0.49%	–	52.9%

Therefore, even with this limitation, it is possible to reach some conclusions when comparing the solution presented in this article with the related works.

The work [17], which was evaluated in 3D-HTM 8.1, achieved a

timesaving of 27.9% at the cost of reducing BD-rate in 1.03%. The mode-level and a block-level combined scheme proposed in [18] saves 32.9% of execution time with the increase of 0.54% in BD-rate when evaluated in the 3D-HTM 13.0. The work [19] reduced 37.6% of execution time with an increase of 0.8% in BD-rate. The high timesaving obtained in [19] is mainly related to the early terminate the evaluation at a quadtree-level decision. Our previous work [20] that was used as a base for P&GMOF is the unique solution with gains on encoding efficiency with a small timesaving. It saves only 1.7% of the time with a decrease of 0.047% in BD-rate running in 3D-HTM 7.0. The work [21] reduces the effort spent in DMM-1 in 52.9% with an increase of 0.49% in BD-rate. The work [21] does not show the timesaving obtained for the global encoder. However, it can reduce less the DMM-1 evaluation than both algorithms described in this article. Moreover, its timesaving should be limited to the DMM-1 execution time presented in our analysis.

These results show that the proposed mode-level scheme obtained one of the best results regarding timesaving, losing less than 6% and 1% when compared with works [19] and [18], respectively. Moreover, the BD-rate increase of our solution is much better than [17–19], and [21]. Our work only loses in BD-rate for our previous work [20], which has a low impact on the encoding time. Therefore, one can conclude that our work has the best tradeoff between BD-rate and encoding timesaving among all related works. Moreover, the proposed scheme can still be combined with other timesaving schemes to achieve higher timesaving rates.

7. Conclusions

This article presents a reduced effort mode-level scheme composed of three algorithms: the DMM-1 Fast Pattern Selector (DFPS), the Pattern and Gradient-based Mode One Filter (P&GMOF) and the Enhanced Depth Rough Mode Decision (ED-RMD). This scheme aims to reduce the encoding time of depth maps intra-frame prediction by focusing on the most time-consuming steps, i.e., the DMM-1, TQ and SDC evaluations. Software evaluations in 3D-HTM 16.0 demonstrate that the proposed scheme was able to reduce the entire 3D-HEVC encoder execution time in 31.9%, with a BD-rate increase of 0.272%. Through comparisons with related works, it is possible to conclude that the designed scheme achieves competitive timesaving with the lowest losses in encoding performance; i.e., the proposed scheme has the best tradeoff between timesaving and encoding efficiency losses among all related works.

Acknowledgment

This paper was achieved in cooperation with Hewlett-Packard Brazil Ltda. using incentives of Brazilian Informatics Law (Law n° 8.248 of 1991). Authors also would like to thank CAPES (processes 88881135737/2016-01 and 88881119481/2016-01), CNPq (processes 309707/2015-3 and 486136/2013-2) and FAPERGS (process 16/2551-0000241-0) Brazilian research agencies to support the development of this work.

References

- [1] K. Muller, H. Schwarz, D. Marpe, C. Bartnik, S. Bosse, H. Brust, T. Hinz, H. Lakshman, P. Merkle, F. Rhee, G. Tech, M. Winken, T. Wiegand, 3D high-efficiency video coding for multi-view video and depth data, *IEEE Trans. Image Process.* (TIP) 22 (9) (2013) 3366–3378.
- [2] G. Tech, Y. Chen, K. Muller, J. Ohm, A. Vetro, Y. Wang, Overview of the Multiview and 3D extensions of High Efficiency Video Coding, *IEEE Trans. Circuits Syst. Video Technol.* (TCSVT) 26 (1) (2016) 35–49.
- [3] P. Kauff, N. Atzpadin, C. Fehn, M. Muller, O. Schreier, A. Smolic, R. Tanger, Depth map creation and image-based rendering for advanced 3DTV services providing interoperability and scalability, *Signal Process. Image Commun.* 22 (2) (2007) 217–234.
- [4] K. Muller, A. Vetro, Common Test Conditions of 3DV Core Experiments, ISO/IEC JTC1/SC29/WG11 MPEG2011/N12745, San José, US, 2014.
- [5] P. Merkle, K. Muller, D. Marpe, T. Wiegand, Depth Intra Coding for 3D Video based on Geometric Primitives, *IEEE Trans. Circuits Syst. Video Technol.* (TCSVT) 26 (3) (2015) 570–582.
- [6] J. Lee, M. Park, C. Kim, 3D-CE1: Depth Intra Skip (DIS) Mode, Document JCT3V-K0033, Switzerland, Geneva, 2015.
- [7] H. Liu and Y. Chen, “Generic segment-wise DC for 3D-HEVC depth intra coding”, in *Proc. IEEE International Conference on Image Processing (ICIP)*, pp. 3219–3222, 2014.
- [8] Y. Chen, G. Tech, K. Wegner, S. Yea, Test Model 10 of 3D-HEVC and MV-HEVC, ISO/IEC JTC1/SC29/WG11, Strasbourg, France, 2014.
- [9] D. Marpe, H. Schwarz, S. Bosse, B. Bross, P. Helle, T. Hinz, H. Kirchhoffer, H. Lakshman, T. Nguyen, S. Oudin, M. Siekmann, K. Suhring, M. Winken, T. Wiegand, Video compression using nested quadtree structures, leaf merging, and improved techniques for motion representation and entropy coding, *IEEE Trans. Circuits Syst.* 20 (12) (2010) 1676–1687.
- [10] G. Sullivan, J. Ohm, W. Han, T. Wiegand, Overview of the high efficiency video coding (HEVC) standard, *IEEE Trans. Circuits Syst. Video Technol.* (TCSVT) 22 (12) (2012) 1649–1668.
- [11] Z. Gu, J. Zheng, N. Ling, P. Zhang, Fast Intra Prediction Mode Selection for Intra Depth Map Coding, ISO/IEC JTC1/SC29/WG11, Austria, Vienna, 2013.
- [12] Z. Gu, J. Zheng, N. Ling, P. Zhang, Fast Intra SDC Coding for 3D-HEVC Intra Coding, ISO/IEC JTC 1/SC 29/WG 11, Sapporo, Japan, 2014, pp. 3–9.
- [13] J. Lainema, F. Bossen, W. Han, J. Min, K. Ugur, Intra coding of the HEVC standard, *IEEE Trans. Circuits Syst. Video Technol.* (TCSVT) 22 (12) (2012) 1792–1801.
- [14] L. Zhao, L. Zhang, S. Ma, D. Zhao, “Fast Mode Decision Algorithm for Intra Prediction in HEVC”, in *Proc. IEEE Visual Communications and Image Processing (VCIP)*, pp. 300–304, 2011.
- [15] X. Zhao, L. Zhang, Y. Chen, M. Karczewicz, “CE6.h related: Simplified DC predictor for depth intra”, in: Joint Collaborative Team on 3D Video Coding Extensions (JCT-3V) document JCT3V-D0183, 4th JCT-3V Meeting: Incheon, Korea, Apr. 2013.
- [16] M. Budagavi, A. Fuldseth, G. Bjontegaard, HEVC transform and quantization, in: V. Sze, M. Budagavi, G. Sullivan (Eds.), *High Efficiency Video Coding (HEVC): Algorithms and Architectures*, Springer, 2014.
- [17] H. Zhang, C. Fu, Y. Chan, S. Tsang, W. Siu, “Efficient depth intra mode decision by reference pixels classification in 3D-HEVC”, in: *Proc. IEEE International Conference on Image Processing (ICIP)*, pp. 961–965, 2015.
- [18] H. Zhang, S. Tsang, Y. Chan, C. Fu, W. Su, “Early determination of intra mode and segment-wise DC coding for depth map based on hierarchical coding structure in 3D-HEVC”, in: *Proc. Asia-Pacific Signal and Information Processing Association Annual Summit and Conference (APSIPA)*, pp. 374–378, 2015.
- [19] K. Peng, J. Chiang, W. Lie, “Low complexity depth intra coding combining fast intra mode and fast CU size decision in 3D-HEVC”, in: *Proc. IEEE International Conference on Image Processing (ICIP)*, pp. 1126–1130, 2016.
- [20] G. Sanchez, M. Saldanha, G. Balota, B. Zatt, M. Porto, L. Agostini, “A Complexity reduction algorithm for depth maps intra prediction on the 3D-HEVC”, in: *Proc. Visual Communications and Image Processing (VCIP)*, pp. 137–140, 2014.
- [21] C. Fu, H. Zhang, W. Su, S. Tsang, Y. Chan, “Fast wedgelet pattern decision for DMM in 3D-HEVC”, in: *Proc. IEEE International Conference on Digital Signal Processing (DSP)*, pp. 477–481, 2015.
- [22] G. Sanchez, L. Agostini, C. Marcon, “3D-HEVC depth maps intra prediction complexity analysis”, in: *Proc. IEEE International Conference on Electronics, Circuits, & Systems (ICECS)*, pp. 1–4, 2016.
- [23] G. Sanchez, L. Jordani, L. Agostini, C. Marcon, DFPS: a fast pattern selector for depth modeling mode 1 in three-dimensional high-efficiency video coding standard, *J. Electron. Imaging* (JEI) 25 (6) (2016) 063011.
- [24] G. Sanchez, L. Agostini, C. Marcon, “Complexity reduction by modes reduction in RD-list for intra-frame prediction in 3D-HEVC depth maps”, in: *International Symposium on Circuits and Systems (ISCAS)*, 2017.
- [25] G. Bjontegaard, Calculation of Average PSNR Differences between RD curves, ITU-T SC16/SG16 VCEG-m33, Austin, US, 2001.

Gustavo Sanchez is Professor at the IFFarroupilha, Brazil, since 2014. Sanchez received the Electrical Engineer degree from the Sul-Rio-Grandense Federal Institute of Education, Science and Technology (2013) and B.S. degree in Computer Science from the Federal University of Pelotas (2012). In 2014, he received his M.Sc. degree in Computer Science from the Federal University of Pelotas. Sanchez is currently pursuing his Ph.D. degree in Computer Science at the Pontifical Catholic University of Rio Grande do Sul. He has 9+ years of research experience on algorithms and hardware architectures for video coding. His research interests include fast encoding algorithms, hardware-friendly algorithms and dedicated hardware design for 2D and 3D video coding.

Luciano V. Agostini is a Professor since 2002 at Federal University of Pelotas (UFPEL), Brazil, where he leads the Video Technology Research Group (ViTech) and the Group of Architectures and Integrated Circuits (GACI). He received the M.S. and Ph.D. degrees from Federal University of Rio Grande do Sul, Brazil, in 2002 and 2007 respectively. Since 2013 he is a distinguished Brazilian researcher granted by CNPq agency. From 2013 to 2016, he was the Executive Vice President for Research and Graduate Studies of UFPEL. He has more than 200 published papers in journals and conference proceedings. His research interests include 2D and 3D video coding, algorithmic optimization, arithmetic circuits, FPGA based design and microelectronics. Dr. Agostini is a Senior Member of IEEE and a member of the IEEE CAS, CS, and SPS societies. He is a member of the Multimedia Systems & Applications Technical Committee (MSATC) at the IEEE CAS. He is also Senior Member of ACM, and member of SBC and SBMicro Brazilian societies.

César Marcon is Professor at the School of Computer Science of Pontifical Catholic University of Rio Grande do Sul (PUCRS), Brazil, since 1995. He received his Ph.D. in Computer Science from Federal University of Rio Grande do Sul, Brazil, in 2005. Professor Marcon is member of the Institute of Electrical and Electronics Engineers (IEEE) and of the Brazilian Computer Society (SBC). He is advisor of MsC. and Ph.D. graduate students at Graduate Program in Computer Science of PUCRS. He has more than 100 papers

published in prestigious journals and conference proceedings. Since 2005, prof. Marcon coordinated nine research projects in areas of telecom, healthcare, and telemedicine. His research interests are in the areas of embedded systems in the telecom domain, MPSoC architectures, partitioning and mapping application tasks, fault-tolerance and real-time operating systems.